

The Fano-Rashba effect

Llorenç Serra^{1,2} and David Sánchez¹

¹ Departament de Física, Universitat de les Illes Balears, E-07122 Palma de Mallorca, Spain

² Institut Mediterrani d'Estudis Avançats IMEDEA (CSIC-UIB), E-07122 Palma de Mallorca, Spain

E-mail: llorens.serra@uib.es, david.sanchez@uib.es

Abstract. We analyze the linear conductance of a semiconductor quantum wire containing a region where a local Rashba spin-orbit interaction is present. We show that Fano lineshapes appear in the conductance due to the formation of quasi bound states which interfere with the direct transmission along the wire, a mechanism that we term the Fano-Rashba effect. We obtain the numerical solution of the full Schrödinger equation using the quantum-transmitting-boundary method. The theoretical analysis is performed using the coupled-channel model, finding an analytical solution by ansatz. The complete numerical solution of the coupled-channel equations is also discussed, showing the validity of the ansatz approach.

1. Introduction

The spin-orbit (SO) interactions in semiconductor nanostructures are currently attracting much interest due to their central role in the characterization and control of spin properties of these systems [1]. Particular attention is devoted to the Rashba interaction in two-dimensional quantum wells —a SO coupling stemming from the well inversion asymmetry in the growth direction whose intensity can be manipulated by electrical gating [2, 3]. The Rashba interaction is also the underlying physical mechanism for the operation of the proposed spin transistor, one of the paradigms of spintronic device, exploiting the electron's spin to control the charge current between two ferromagnetic contacts [4].

In a quantum wire with *uniform* SO interaction the energy subbands deviate from the simple parabolic behavior, with band splittings and anticrossings that yield a modified wire conductance and the possibility of spin-textured states [5]. In this work we consider a wire with *nonuniform* Rashba interaction, localized to a finite region acting as a spin scattering center (a Rashba dot) that affects the wire conductance properties. It will be shown with numerical and analytical results that this geometry leads in a natural way to the appearance of Fano resonance profiles in the energy dependence of the conductance that depend quite sensitively on the properties of the Rashba dot, such as its dimensions and SO intensity. We refer to this influence of the Rashba SO coupling on the wire conductance as the Fano-Rashba effect.

Fano resonances [6] are a general phenomenon that has been observed in different fields, such as atomic physics [7], Raman scattering [8] and mesoscopic electron transport [9]. Fano-resonance physics appears wherever there is an interference between two paths, one corresponding to direct transmission and the other to the passage through a quasi-bound state lying nearby in energy. As a consequence, characteristic asymmetric lineshapes appear in the most general case, with conductance dips in which transmission is greatly quenched. Indeed, for

the case of scattering centers that may be modelled as attractive potentials it was shown that an exact transmission zero should always be present [10, 11]. In our case of a Rashba dot the existence of transmission zeros is not always guaranteed and only for some specific dimensions and intensities of SO coupling the wire conductance vanishes at the dip position.

A useful theoretical framework to understand Fano resonances is the coupled-channel model (CCM). In this approach the wave function is approximated by the superposition of different channel components, each of them obeying an equation containing the channel background contribution and also the coupling with the other channels. We shall compare the prediction of CCM with the exact numerical solution obtained from a grid discretization of the Schrödinger equation. The prediction of the CCM will be analyzed using the ansatz for the quasi-bound state channel proposed by Nöckel and Stone [11], and also with a full numerical solution of the CCM equations. In this way we shall explicitly proof the validity of the ansatz. This analysis is an extension of our recent work [12] and is also related to the study in Ref. [13] where numerical results for the transmission of wires with a modulated Rashba intensity were obtained. A localized Rashba interaction in a quantum wire was also considered in Ref. [14] for the study of shot noise and entanglement within a beam splitter configuration.

2. The physical system

2.1. Hamiltonian

We assume the effective-mass model for the conduction band states of a two-dimensional electron gas in GaAs and consider a parabolic confinement in the y direction, yielding a ballistic quantum wire along x . The system Hamiltonian reads

$$H = \frac{p_x^2 + p_y^2}{2m} + \frac{1}{2}m\omega_0^2 y^2 + H_R. \quad (1)$$

The oscillator is used to define our energy $\hbar\omega_0$ and length $\ell_0 = \sqrt{\hbar/m\omega_0}$ units. The Rashba Hamiltonian H_R that we consider in Eq. (1) is characterized by an intensity $\alpha(x)$ vanishing everywhere except for $0 < x < \ell$ where it takes the value α_0 .¹ In detail, H_R reads

$$H_R = \frac{\alpha(x)}{2\hbar} (p_y\sigma_x - p_x\sigma_y) + h.c., \quad (2)$$

where σ_x and σ_y are the Pauli matrices and the Hermitian conjugation is used to ensure Hermiticity. The inset to Fig. 1 shows a simple sketch of the physical system under consideration.

2.2. Localized states in ballistic transport

We have obtained the linear conductance \mathcal{G} as a function of the electron energy (Fermi energy) discretizing the xy plane in a uniform grid and using the quantum-transmitting-boundary algorithm [15]. This method transforms the Schrödinger equation into a complex linear system whose dimension is twice the number of grid points, due to the two spin components. In spite of the typically large dimension, the system is highly sparse and it can be solved efficiently with standard numerical routines. This approach provides the exact wave function for the ballistic transport problem from which one obtains the transmission amplitudes and the wire's linear conductance.

Figure 1 shows a typical conductance curve for specific values of α and ℓ . The usual staircase conductance is modified because of the Rashba dot in two main aspects. First the initial part of the step is smoothed, a usual quantum behavior of scattering through potential wells. The

¹ In the numerical applications we take $\alpha(x) = \alpha_0[f(x - \ell) - f(x)]$, with $f(x) = 1/(1 + e^{x/\sigma})$ and σ a small diffusivity. The results are not very sensitive to the precise value of σ provided $\sigma < \ell$.

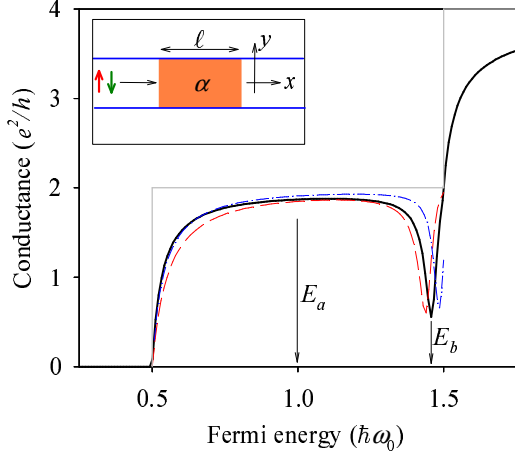


Figure 1. (Color online) Conductance for a Rashba dot of $\ell = \ell_0$ and $\alpha_0 = 0.75\hbar\omega_0\ell_0$ in the exact (solid), numerical CCM (dashed) and analytical CCM (dash-dotted) calculations. The solid gray line shows the case without Rashba dot and the inset sketches the physical system.

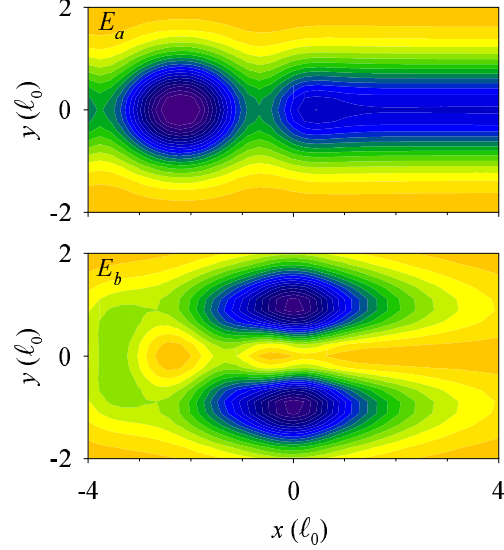


Figure 2. (Color online) Probability densities for the energies E_a (upper) and E_b (lower) indicated in Fig. 1. Darker means higher probability.

second conspicuous feature is the existence of a pronounced conductance dip near the end of the conductance plateau. It was already mentioned that the existence of conductance dips is normally due to quasibound states. To proof it in the present context we show in Fig. 2 the wave function for two different energies, E_a and E_b , where E_a is chosen to lie in the smooth conductance region while E_b corresponds precisely to the dip position. Indeed, at energy E_b the wave function strongly resonates within the Rashba dot, being so amplified that it greatly exceeds the values in the leads. This explicitly shows the dramatic influence of the quasibound state. A systematic analysis of the dip positions for varying α 's and ℓ 's was performed in Ref. [12].

3. The coupled channel model

3.1. Channel equations

The physics behind the results shown in the preceding section is more easily analyzed within the CCM. Assume the following expansion of the electron wave function $\Psi(x, y, \eta)$, with $\eta = \uparrow, \downarrow$, in the transverse oscillator modes $\phi_n(y)$, with energies ε_n , and spin eigenstates $\chi_{\pm}(\eta)$ of σ_y ,

$$\Psi(x, y, \eta) = \sum_{n,s=\pm} \psi_{ns}(x)\phi_n(y)\chi_s(\eta). \quad (3)$$

Substituting Eq. (3) into the Schrödinger equation $H\Psi = E\Psi$ and projecting onto the functions $\phi_n\chi_s$ we obtain the CCM equations for the different channel amplitudes $\psi_{ns}(x)$. We shall restrict to the first conductance plateau, i.e., to electron energies fulfilling $\varepsilon_1 < E < \varepsilon_2$ and also truncate the expansion in Eq. (3) to the first two transverse modes $n = 1, 2$. The selection rules stemming from the Rashba interaction require spin flip and also $\Delta n = \pm 1$. Therefore we obtain two independent two-band models, with ψ_{1+} coupled to ψ_{2-} and ψ_{1-} to ψ_{2+} . Actually, the two models are equivalent and we shall focus for simplicity on the $\psi_{1+}-\psi_{2-}$ system.

The CCM equations for the ψ_{1+}, ψ_{2-} amplitudes are greatly simplified by means of the following gauge transformation $\psi_{1+,2-} \rightarrow \psi_{1+,2-} \exp(\pm i \int^x k_R(x') dx')$, where we have defined

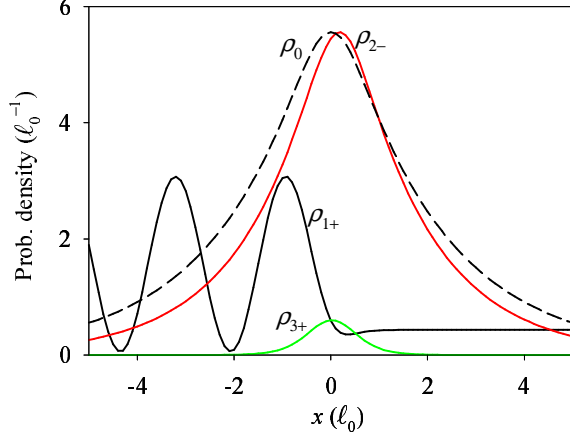


Figure 3. (Color online) Channel probability densities within CCM, defined as $\rho_{ns}(x) = |\psi_{ns}(x)|^2$, for the energy E_b of Fig. 1. The probability density corresponding to the background bound state $\rho_0(x) = |\phi_0(x)|^2$ is also shown. $\rho_0(x)$ has been arbitrarily rescaled in order to reproduce the peak height of $\rho_{2-}(x)$ for better comparison.

$k_R(x) = m\alpha(x)/\hbar^2$. The resulting CCM system then reads

$$\left[\frac{p_x^2}{2m} - \frac{\hbar^2 k_R(x)^2}{2m} - E + \varepsilon_1 \right] \psi_{1+}(x) = V_{12}(x) \psi_{2-}(x), \quad (4)$$

$$\left[\frac{p_x^2}{2m} - \frac{\hbar^2 k_R(x)^2}{2m} - E + \varepsilon_2 \right] \psi_{2-}(x) = V_{21}(x) \psi_{1+}(x). \quad (5)$$

The left hand sides of Eqs. (4) and (5) constitute the channel background problems. They are 1D Schrödinger equations for a potential well $-\hbar^2 k_R(x)^2/2m$ with the only difference that the energy is positive (negative) for ψ_{1+} (ψ_{2-}). This clearly shows the propagating and evanescent character of the two channels, respectively. The right-hand-sides contain the channel couplings, with the mixing potentials

$$V_{12}(x) = V_{21}^*(x) = \frac{i}{\hbar} \langle \phi_1 | p_y | \phi_2 \rangle \alpha(x) e^{2i \int^x k_R(x') dx'}. \quad (6)$$

3.2. Ansatz solution

The evanescent character of ψ_{2-} in Eq. (5) motivates the ansatz $\psi_{2-}(x) \propto \phi_0(x)$, where ϕ_0 is the background bound state fulfilling $(p_x^2/2m - \hbar^2 k_R^2/2m - \varepsilon_0) \phi_0 = 0$, with $\varepsilon_0 < 0$. Since $E > \varepsilon_1$, Eq. (4) describes a 1D scattering process with a source term given by $V_{12}\psi_{2-}$ and asymptotic wave vector $k = \sqrt{2m(E - \varepsilon_1)/\hbar^2}$. Using the Green function G , given in terms of the background asymptotic states φ_r and φ_l behaving as $te^{\pm ikx}$ for $x \rightarrow \pm\infty$, respectively, we find the total transmission,

$$T_+(E) = |t|^2 \frac{(E - \varepsilon_2 - \varepsilon_0 - \Delta + \delta)^2 + (\gamma - \Gamma)^2}{(E - \varepsilon_2 - \varepsilon_0 - \Delta)^2 + \Gamma^2} \equiv |t|^2 \frac{|\epsilon + q|^2}{\epsilon^2 + 1}. \quad (7)$$

We have defined $\Delta + i\Gamma \equiv \langle \phi_0 | V_{21} G V_{12} | \phi_0 \rangle$, $\delta + i\gamma \equiv \frac{m}{i\hbar^2 k t} \langle \varphi_l^* | V_{12} | \phi_0 \rangle \langle \phi_0 | V_{21} | \varphi_r \rangle$ and the last expression in Eq. (7) corresponds to the generalized Fano lineshape, with $\epsilon = (E - \varepsilon_2 - \tilde{\varepsilon}_0)/\Gamma$ and $q = \delta/\Gamma + i(\gamma/\Gamma - 1)$. In general, the Rashba dot yields complex q 's and therefore the factor $|\epsilon + q|$ in Eq. (7) can not exactly vanish at any E , thus hindering the formation of zero transmission dips. For some particular values of α and ℓ , however, we showed in Ref. [12] that there are *accidental* cases where the conductance dip is compatible with a zero value within numerical precision. As shown by the dash-dotted line of Fig. 1, the ansatz solution satisfactorily reproduces the conductance dip although, of course, there are some minor discrepancies with the exact solution of the preceding section (solid line).

3.3. Numerical solution

The exact solution of the CCM equations can also be obtained numerically, avoiding the ansatz, using a 1D formulation of the quantum-transmitting-boundary algorithm. Dashed line in Fig. 1 corresponds to the conductance obtained from this numerical CCM approach while Fig. 3 shows the different channel amplitudes (including also the ψ_{3+} channel), as well as the bound state ϕ_0 , for the dip energy E_b of Fig. 1. The probability density for channel ψ_{1+} again proves the propagating character of this channel although transmission is rather low at this energy. There is good qualitative agreement of the probability densities ρ_{2-} and ρ_0 , explicitly proving that the ansatz is indeed a reasonable assumption for the evanescent channels. The numerical solution has been obtained including also channel ψ_{3+} , however, the smallness of ρ_{3+} with respect to the other channel densities supports the truncation to the lowest two modes of the preceding subsection.

4. Conclusions

We have theoretically investigated the influence of a localized Rashba scattering center (a Rashba dot) on the linear conductance of a quantum wire. The Rashba dot sustains quasi-bound states that interfere with the direct transmission along the wire and lead to Fano-resonance profiles in the energy dependence of the linear conductance. This Fano-Rashba effect has been elucidated with numerical calculations using a grid discretization of the 2D Schrödinger equation. We also analyzed a coupled-channel model, finding analytical expressions within the ansatz approach that clearly show the appearance of the Fano function for the transmission. Finally, the validity of the ansatz solution and the truncation to the lowest two modes has been assessed by finding the numerical solution of the multimode coupled-channel-model equations.

Acknowledgments

We acknowledge R. López for valuable discussions. This work was supported by the Grant No. FIS2005-02796 (MEC) and the “Ramón y Cajal” program.

References

- [1] Zutic I, Fabian J and Das Sarma S 2004 *Rev. Mod. Phys.* **76** 323
- [2] Rashba E I 1960, *Fiz. Tverd. Tela* (Leningrad) **2** 1224 [*Sov. Phys. Solid State* **2** 1109]
- [3] Nitta J, Akazaki T, Takayanagi H and Enoki T 1997 *Phys. Rev. Lett.* **78** 1335; Engels G, Lange J, Schäpers Th and Lüth H 1997 *Phys. Rev. B* **55** R1958
- [4] Datta S and Das B 1990 *Appl. Phys. Lett.* **56** 665
- [5] Schäpers Th, Knobbe J and Guzenko V A 2004 *Phys. Rev. B* **69** 235323; Mireles F and Kirczenow G 2001 *Phys. Rev. B* **64** 024426; Governale M and Zülicke U 2002 *Phys. Rev. B* **66** 073311; Serra Ll, Sánchez D and López R 2005 *Phys. Rev. B* **72** 235309
- [6] Fano U 1961 *Phys. Rev.* **124** 1866
- [7] Adair R K, Bokelman C K and Peterson R E 1949 *Phys. Rev.* **76** 308
- [8] Cerdeira F, Fjeldly T A and Cardona M 1973 *Phys. Rev. B* **8** 4734
- [9] Göres J *et al* 2000 *Phys. Rev. B* **62** 2188; Kobayashi K, Aikawa H, Katsumoto S and Iye Y 2002 *Phys. Rev. Lett.* **88** 256806
- [10] Gurvitz S A and Levinson Y B 1993 *Phys. Rev. B* **47** 10578
- [11] Nöckel J U and Stone A D 1994 *Phys. Rev. B* **50** 17415
- [12] Sánchez D and Serra Ll 2006 *preprint cond-mat/0608392*; *Phys. Rev. B* (in press).
- [13] Zhang L, Brusheim P and Xu H Q 2005 *Phys. Rev. B* **72** 045347
- [14] Egues J C, Burkard G and Loss D 2002 *Phys. Rev. Lett.* **89** 176401
- [15] Lent C S and Kirkner D J 1990 *J. Appl. Phys.* **67** 6353